Journal of Zhejiang University SCIENCE A
ISSN 1673-565X (Print); ISSN 1862-1775 (Online)
www.zju.edu.cn/jzus; www.springerlink.com
E-mail: jzus@zju.edu.cn

Novel high torque bearingless two-sided rotary ultrasonic motor*

LI Xia†, CHEN Wei-shan, XIE Tao, LIU Jun-kao

(*Department of Mechatronics Engineering, Harbin Institute of Technology, Harbin 150001, China*)

†E-mail: jennyhit@163.com

Received May 10, 2006; revision accepted Sept. 15, 2006

Abstract: Applications are limited at present because the currently available ultrasonic motors (USMs) do not provide sufficiently high torque and power. The conventional travelling-wave USM needs the bearing to support, which required lubricant. To solve the above problem, a bearingless travelling-wave USM is designed. First, a novel structure of the two-sided USM consisting of a two-sided teeth stator and two disk-type rotors is designed. And the excitation principle of the two-sided travelling-wave USM is analyzed. Then, using ANSYS software, we set up the model of the stator to predict the excitation frequency and modal response of the stator. The shape of the vibration mode was obtained. Last, the load characteristics of the USM are measured using experimental method. The maximum stall torque and the no-load speed were obtained. The results showed that the characteristics of the two-sided USM are better than those of the conventional one-sided USM.

Key words: Two-sided, Ultrasonic motor (USM), Piezoelectric motor, Travelling-wave, Bearingless
doi:10.1631/jzus.2007.A0786 **Document code:** A **CLC number:** TM356; TM359.6

INTRODUCTION

Ultrasonic motors (USMs) have excellent performance and many useful features such as high holding torque, high torque at low speed, quiet operation, simple structure, compactness, and no electromagnetic interferences (Kanda *et al*., 2006; Chen *et al*., 2006). It may be widely used as actuators for robots, cameras, precise positioning devices, machines in space and medical treatment devices (Bar-Cohen *et al*., 1998; Hagood and McFarland, 1995). However, applications are limited at present because the currently available USMs do not provide sufficiently high torque and power. Previous studies for increasing torque and power of USM mainly focused on standing wave type and hybrid-transducer type motor (Kurosawa *et al*., 1998; Xu *et al*., 2005; Guo and Wu, 2004). Although these motor types are expected to produce higher torque, they are likely to become larger in size. To solve the above problem, a two-sided high torque travelling-wave USM is designed. In contrast to the typical configuration of conventional travelling-wave USMs with a single contact interface of an asymmetric stator, the two-sided motor has dual contact interfaces of a symmetric stator. The main purpose of two-sided operation is to maximize the output torque of a given motor package, inherently increasing achievable torque densities (torque per unit mass) and enabling reduced mass and size compared to one-sided designs (Glenn and Hagood, 1997).

The integration of two-sided operation is specifically intended to expand the practicality of direct drive by increasing the available torque at lower operating speeds and to improve the potential for smaller, lighter-weight assemblies. Existing one-sided designs provide the means for compact, direct-drive actuation of many limited torque applications, but there is a growing demand for the benefits of USMs in high-torque robotics and automobile applications and a need to improve the temperature range of operation for space missions. Also, two-sided operation is expected to yield greater effi-

* Project (No. 50175018) supported by the National Natural Science Foundation of China

ciencies than single-sided operation, and the built-in symmetric aspects of the two-sided motor should contribute to thermal stability. Petit *et al*.(2001) even went as far as testing their stators with two rotors, similar to the two-sided implementation of the disk motor by (Glenn and Hagood, 1997). Kawai *et al*.(1995) and Jin *et al*.(1998) also designed a two-sided travelling-wave USM. Their results clearly supported the two-sided piezoceramic travelling-wave USM that produced approximately twice as high maximum torque and output power with little added mass, as the conventional USM employing a piezoceramic of the same diameter and the same resistive resin material (Glenn and Hagood, 1997; Kawai *et al*., 1995; Jin *et al*., 1998).

The conventional travelling-wave USM needs the bearing to support, which required lubricant. The application of USM on aeronautics and space is limited. In our research, we design a bearingless two-sided piezoelectric travelling-wave USM, and clarify the principle of motion of the travelling-wave motor and the driving method of flexible wave. Finite element method (FEM) was used to analyze the vibration mode of the two-sided teeth stator of the travelling-wave USM. The load characteristics of USM were measured using experimental method. The maximum stall torque of the two-sided travelling-wave USM was obtained. Experiment results showed that the characteristics of the two-sided USM are better than those of the conventional USM.

STUDY OF THE TWO-SIDED USM

Motor structure

The rotors of the two-sided USM fabricated by Glenn (2002), are fixed, and the stator turns. The USM needs the brush to deliver quadriture voltage signals to the rotating frame of the piezoceramics. The signal noise generated at the brush contact is not negligible. In this paper, the shaft of the stator is fixed, the two rotors rotate.

The configuration of the two-sided USM shown in Fig.1 consists of a dual teeth stator, two rotors, frictional material and six bolts. The heart of the piezoelectric travelling-wave rotary USM is the stator, a comb-toothed structure, bonded by two piezoceramics for exciting a travelling-wave about its circumference. There are sixty 2 mm thick teeth on each side of the stator. The teeth provide a means for increasing the thickness of the stator for greater amplification of the transverse surface displacements with significantly increasing flexural stiffness, and also disperse the dust created by friction and keep the contact surface clean. The stator is near the rotor. The interface between the stator and the rotor is conical surface, which can support the rotor without using bearing. The friction material sticking on the conical surface of the rotor can ensure good pre-elasticity and large radial stiffness when the cone-shaped surface contacts the stator. Bolts are used to connect the rotors and stator, provide the pretightening force between the rotors and the toothed stator. Between the rotors and bolts are rubber shims to allow variable preload. The leads welded on piezoceramics are connected with wire leading out through holes machined in the stator shaft.

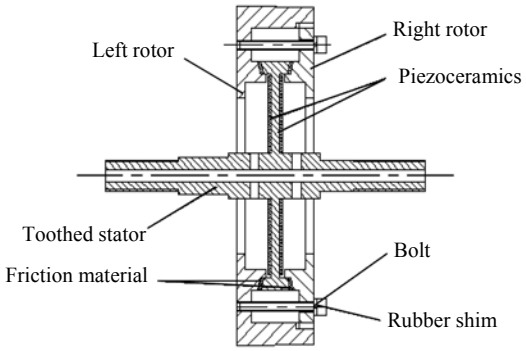

Fig.1 Structure of the ultrasonic motor

There are two piezoceramics bonded to each side of the two-sided stator for exciting a travelling-wave about its circumference. PZT8, whose size parameter is ∅60 mm×∅16 mm×1 mm was chosen to excite the travelling-wave.

Working principle

The speed and torque of a piezoelectric travelling-wave rotary USM are derived from frictional contact forces acting at the interface of the two bodies, one of which has a travelling flexural wave excited about its circumference by piezoceramics. The displacements at the surface of the excited body follow elliptical trajectories, the velocity of which is horizontal, or in-plane, at the peaks of the wave. Typically, the piezoelectrically driven vibrating element is the

stator, and the passive component pressed into contact with the stator is the rotor, driven into rotary motion by the tangential forces at the contact surface.

A blown in Fig.2 shows the relative motion of the wave and the tips of the teeth. As the travelling-wave propagates around the circumference of the vibrating structure, the teeth have elliptical trajectories with only a horizontal component of velocity at the peaks and valleys of the wave. USMs of the rotary travelling-wave type are typically driven near resonance in the tens of kilohertz (above the 20 kHz limit of human hearing) generating wave amplitudes in the order of microns. The effect of coupling a rotor to the peaks of the wave is to rectify the microscopic displacements of the stator into a continuous rotary stroke of either the rotor(s) or the stator itself. Note that the direction of motion of the wave is opposite that of the relative velocity between the rotor and stator, with respect to the frame of the stator. Also, the propagation direction of the wave, and thus the rotation direction of the rotor, may be reversed by inverting the voltage phase on either of the piezoelectric arrays (Glenn and Hagood, 1997; Glenn, 2002).

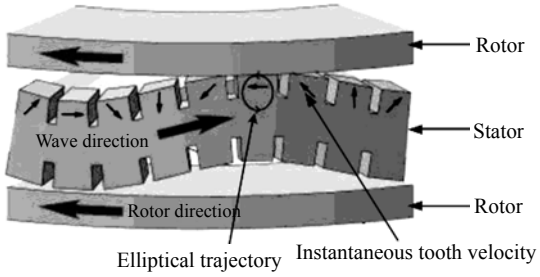

Fig.2 Principle of motion illustrating of the travelling-wave motor (Glenn, 2002)

As illustrated in Fig.3, excitation of the travelling-wave is typically realized by the phased superposition of two standing waves. Two piezoelectric arrays, bonded to the upper and lower surfaces of the stator and identified in the figure as A and B are etched and poled so as to spatially coincide with the desired pair of orthogonal degenerate modes of circumferential wavelength λ. Specifically, each array consists of segments of width $\lambda/2$ and alternating polarization, with the two arrays being offset from one another by $\lambda/4$.

Phase A is driven with $V_0\sin\omega t$ and Phase B with $V_0\cos\omega t$. The displacement on each piezoceramic is

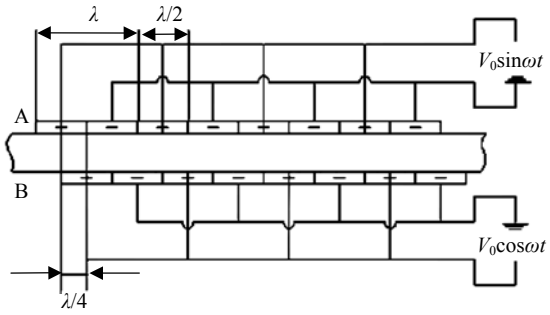

Fig.3 Driving method of flexible travelling-wave

$$y_1 = V_0 \sin\omega t \sin n\theta, \tag{1}$$

$$y_2 = V_0 \cos\omega t \cos n\theta, \tag{2}$$

where V_0, θ, ω and t respectively refer to the amplitude, phase angle, vibration frequency and vibration time. $n=\omega/v=2\pi/\lambda$ describes the wave number on the stator circumference.

Then, mathematically, how a travelling-wave is derived from orthogonal standing waves can be described by the trigonometric identity

$$\begin{aligned} y &= y_1 + y_2 \\ &= V_0 \sin\omega t \sin n\theta + V_0 \cos\omega t \cos n\theta \\ &= V_0 \cos(n\theta - \omega t). \end{aligned} \tag{3}$$

This expression is just that of one of the travelling flexible waves. That is to say the flexible travelling-wave is formed by two-resonance modes of $\pi/2$ phase difference in time and space.

FINITE ELEMENT MODEL

ANSYS finite element modal analysis was used as a final design tool to validate the expected modal frequencies and also to guarantee that other modes do not interfere with the generation of the travelling-wave (Duan *et al*., 2005; Frangi *et al*., 2005). The stator vibration modal of the ring-type USM was calculated by using the simple bending model of a bar (Juang and Gu, 2003). The actual stator of the two-sided travelling-wave USM has a complex shape. As the cross section of the stator is conical surface with two-sided teeth, it is difficult to predict the shape of the stator travelling-wave. So, we calculate the

stator vibration modal by using FEM.

ANSYS 9.0 FEM analytical software was used to deal with the vibration modal of unitary PZT and the stator. Here, the function of the PZT is electro-static-structural conversion. So the element of PZT chooses finite element SOLID227 that support the coupled-field. In coupled-field analysis, the two PZT can be looked on as double piezoelectric films in order to get resonance frequency of the USM. The electric boundary condition is short circuit (resonance) case. For the short-circuit case the top and bottom electrodes are grounded (voltages are set equal to zero).

The performance of USMs is related to the choice of the vibration mode. As the stator was ideally simply fixed, we choose the vibration modal of no nodal circle, which is beneficial for the work of USMs. So (6, 0) vibration modal is chosen here.

The ideal track of driving particles of the stator is planar elliptical track in the circumferential tangent direction. This ideal track will occur only when the position of the stator teeth is designed on the wave amplitude of the preferentially chosen vibration mode. Otherwise, one side of the tangent driving function of driving particles of the stator weakens; another side of the real track has radial vibration that will produce no power friction. So the teeth are designed on the outer circumference of the stator. In order to ensure the coherence of different driving particles, teeth number ought to be divided exactly by the wave number. The teeth number is 60.

Fig.4 is the third vibration modal, the vibration frequency of which is 22.19 kHz. The difference of this result with the practically driving resonance frequency of 21.59 kHz is in 3% error range.

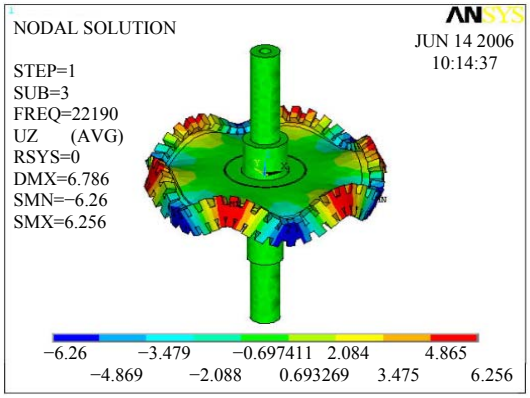

Fig.4 The third vibration mode of the stator

ANALYSIS OF RESONANCE STATE PERFORMANCE

A prototype motor was fabricated. The stator diameter, right rotor diameter and left rotor diameter were respectively 70 mm, 90 mm and 100 mm. The stator was made of steel. The rotor was made of aluminum. Modified polytetrafluoroethylene as frictional material is adhered to the rotor's frictional surface. Fig.5 is the photo of the prototype motor.

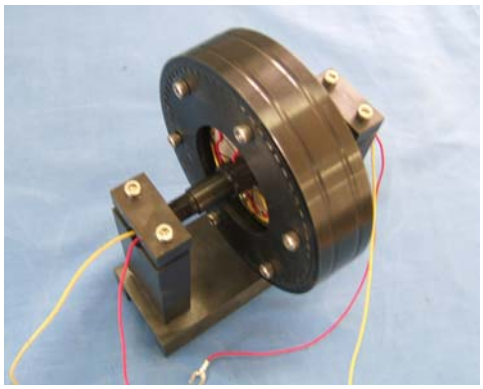

Fig.5 Prototype motor's photo

Before the motor was assembled, the input impedance characteristic of the motor was measured using impedance analyzer (4294 A, Agilent Inc.) at $0.5V_{\mathrm{RMS}}$. Fig.6 and Fig.7 show the measured results in which curves *A* and *B* illustrate the impedance and phase variation versus exciting signal frequency. The frequency of the two piezoceramics has little difference, but it is in the range accepted. In the resonance state, the piezoceramic is pure resistor with minimum resistor value. The measured results above being different from FEM calculated results is mainly caused by the FEM simulation errors, such as the inaccuracy of the material property parameters between the real and simulation ones, neglecting of the epoxide resin, etc.

EXPERIMENT AND RESULTS

Experiment platform

A schematic of the drive electronics is illustrated in Fig.8. Fig.9 is the photo of experiment platform. Quadrature sinusoids were generated by a wave function generators acting in tandem with a master

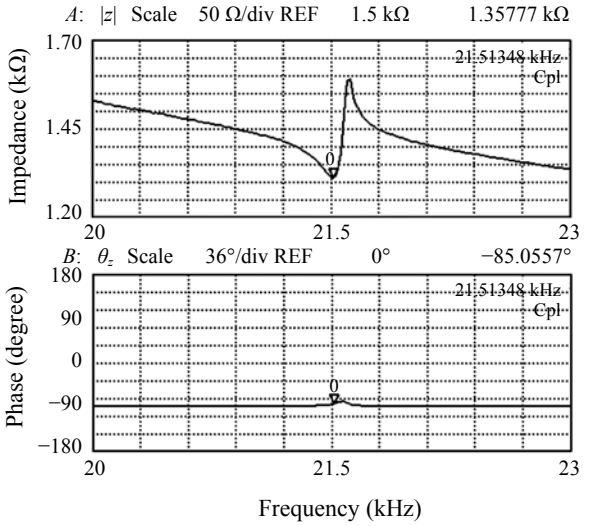

Fig.6 The resonance frequency of the first driving PZT

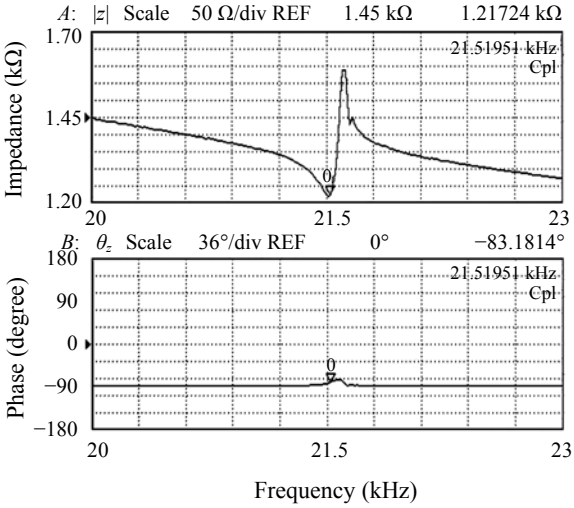

Fig.7 The resonance frequency of the second driving PZT

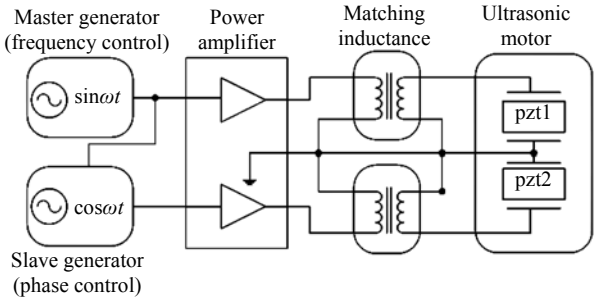

Fig.8 Schematic diagram of driving-circuit

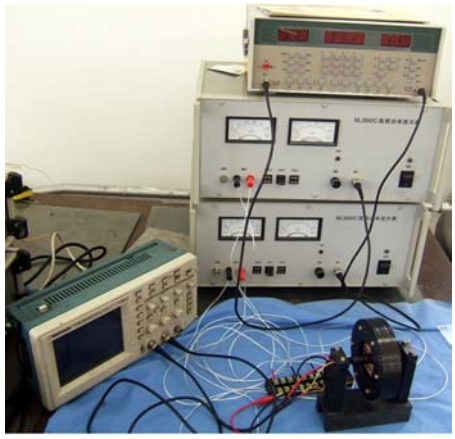

Fig.9 Experiment platform photo

and a slave. The master generator provided digital control of the drive frequency of both waveforms, whereas the slave generator was configured in phase-lock mode and triggered by the master to provide analog control of the phase difference between the two waveforms. The two signals were then amplified by an ML3860C high power stereo amplifier followed by a pair of ML2102 digital inductance.

Mechanical output characteristics

A preload of 5 N was applied on the motor to generate driving friction force. Applied driving voltage was V=150V_{pp} with phase difference of the two input signals being 90 degrees, we adjusted the driving frequency from 21.35 kHz to 21.85 kHz and measured the motor speed. The relationships are shown in Fig.10. It can be concluded that the best working frequency was 21.59 kHz. Under the preload of 5 N, the motor reached its maximum speed of 76 r/min when there was no mechanical load. The figure shows that the practical resonance frequency of 80 Hz is bigger than that before the motor was assembled.

The load characteristics of the motor were altered by adding weights to the pulley device which dragged the motor through a string. Fig.11 shows the relationships between the motor speed and mechanical load under various preload. Under the condition of driving voltage of 150V_{pp}, the motor achieved its maximum torque of 0.5 N·m. With increasing mechanical load, the speed fell sharply as the preload cannot supply enough normal force for the driving friction force and slipping occurred between the driving tip and slider. With increasing of preload, the mechanical output force increased, while the speed decreased.

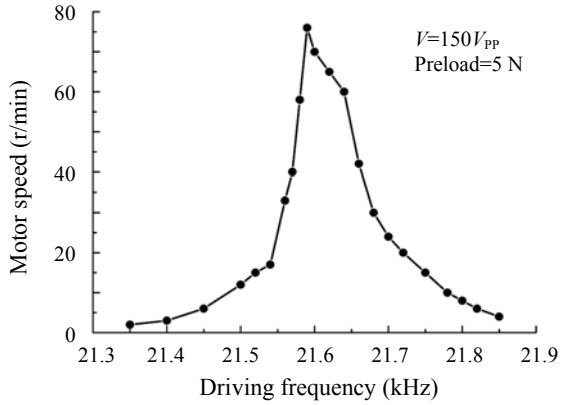

Fig.10 Velocity-frequency curve

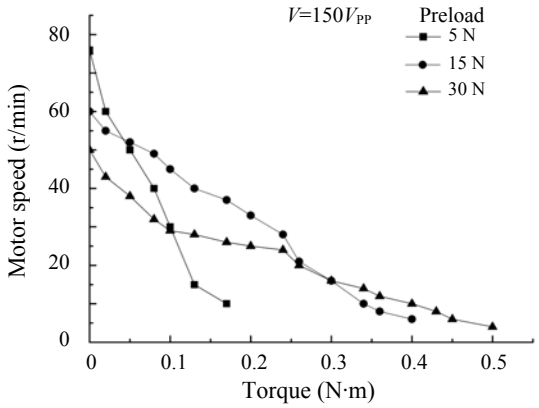

Fig.11 Velocity-torque curves

Table 1 compares the conventional USM by Hao and Chen (2006) and the two-sided USM in this paper. The two-sided travelling-wave USM produced approximately twice as high maximum torque with little added size as the conventional USM using a piezoceramic of the same diameter.

Table 1 Comparison between the conventional USM and two-sided USM

	Conventional USM	Two-sided USM
Stator diameter (mm)	60	70
PZT8 outer diameter (mm)	60	60
PZT8 thickness (mm)	1	1
Maximum torque (N·m)	0.28	0.50

CONCLUSION

A novel bearingless two-sided travelling-wave USM is proposed. The interface between the stator and the rotor is cone-shaped surface, so the rotors were directly supported without bearing. The two-sided motor can produce a large vibrating force and amplitude because the elastic body of the vibrator is sandwiched by two piezoeramics. The major advantages of the two-sided USM are most definitely improved torque and torque density. By measuring the load characteristics of the prototype motor, the maximum no-load speed of the motor reached 76 r/min, and its maximum stall torque reached to 0.5 N·m. In robotics and space missions where any savings of either mass or size are greatly valued, the USM will be used. Also, the symmetric aspect of the two-sided design promotes thermal stability, making it better suited to harsh environments than other USM.

References

Bar-Cohen, Y., Bao, X., Grandia, W., 1998. Rotary Ultrasonic Motors Actuated by Traveling Flexural Waves. Proceedings of the SPIE International Smart Materials and Structures Conference, San Diego, CA, **3329**:794-780.

Chen, Y., Lu, K., Zhou, T.Y., Liu, T., Lu, C.Y., 2006. Study of a mini-ultrasonic motor with square metal bar and piezoelectric plate hybrid. *Jpn. J. Appl. Phys.*, **45**(5B): 4780-4781. [doi:10.1143/JJAP.45.4780]

Duan, W.H., Quek, S.T., Lim, S.P., 2005. Finite element analysis of a ring type ultrasonic motor. *Proc. of SPIE*, **5757**:575-586. [doi:10.1117/12.597983]

Frangi, A., Corigliano, A., Binci, M., Faure, P., 2005. Finite element modelling of a rotating piezoelectric ultrasonic motor. *Ultrasonics*, **43**(9):747-755. [doi:10.1016/j.ultras.2005.04.005]

Glenn, T.S., 2002. Mixed-domain Performance Model of the Piezoelectric Traveling-wave Motor and the Development of a Two-Sided Device. Ph.D Thesis, MIT.

Glenn, T.S., Hagood, N.W., 1997. Development of a two-sided piezoelectric rotary ultrasonic motor for high torque. *Proceedings of SPIE*, **3041**:326-338. [doi:10.1117/12.275657]

Guo, J.F., Wu, J.G., 2004. Research on the high torque and high precision ultrasonic motor for aerospace application. *Journal of Astronautics*, **25**(1):70-76 (in Chinese).

Hagood, N.W., McFarland, A.J., 1995. Modeling of a piezoelectric rotary ultrasonic motor. *IEEE Transactions on Ultrasonics Ferroelectrics and Frequency Control*, **42**(2): 210-224. [doi:10.1109/58.365235]

Hao, M., Chen, W.S., 2006. Analysis and Design of a Ring-type Traveling Wave Ultrasonic Motor. Proceedings of the 2006 IEEE International Conference on Mechatronics and Automation, Luoyang, China, p.1806-1810. [doi:10.1109/ICMA.2006.257508]

Jin, L., Cheng, Z.H., Wang, F.Q., 1998. A new-type piezo-

electric traveling wave ultrasonic motor with the symmetric two-sided teeth. *Journal of Harbin Institute of Technology*, **30**:264-267 (in Chinese).

Juang, P.A., Gu, D.W., 2003. Finite element simulation for a new disc-type ultrasonic stator. *IEEE Transactions on Ultrasonics Ferroelectrics and Frequency Control*, **50**(4):368-375. [doi:10.1109/TUFFC.2003.1197959]

Kanda, T., Makino, A., Ono, T., Suzumori, K., Morita, T., Kurosawa, M.K., 2006. A micro ultrasonic motor using a micro-machined cylindrical bulk PZT transducer. *Sensors and Actuators A: Physical*, **127**(1):131-138. [doi:10.1016/j.sna.2005.10.056]

Kawai, Y., Asai, K., Naito, S., Fukui, T., Adachi, Y., Handa, N., Ikeda, K., Nojima, T., Tsuda, K., 1995. High power traveling-wave type ultrasonic motor. *Jpn. J. Appl. Phys.*, **34**(part 1):2711-2714. [doi:10.1143/JJAP.34.2711]

Kurosawa, M.K., Takahashi, M., Higuchi, T., 1998. Transducer for high speed and large thrust ultrasonic linear motor using two sandwich-type vibrators. *IEEE Transactions on Ultrasonics Ferroelectrics and Frequency Control*, **45**(5):1180-1195. [doi:10.1109/58.726442]

Petit, L., Gonnard, P., Grehant, B., 2001. A Piezomotor for the Small Actuator Market. Proceedings of the 2000 12th IEEE International Symposium on Applications of Ferroelectrics, **1**:33-36. [doi:10.1109/ISAF.2000. 941507]

Xu, Z.K., Hu, M.Q., Jin, L., 2005. The optimization design of traveling wave type ultrasonic motor with large diameter. *Micromotors*, **38**(2):16-19 (in Chinese).